Study on Flame Merging Behavior in Group Fires

W.G. Weng[1, 3] D. Kamikawa[1] K. Kagiya[2] Y. Fukuda[1] Y. Hasemi[1]
[1] School of Science and Engineering, Waseda University,
Okubo 3-4-1, Shinjuku-ku, Tokyo, 169-8555, Japan
[2] National Institute for Land and Infrastructure Management,
Ministry of Land, Infrastructure and Transport,
Kasumigaseki 2-1-3, Chiyoda, Tokyo, 100-8918, Japan
[3] State Key Laboratory of Fire Science, University of Science and Technology of China,
Hefei, Anhui, P.R. China, 230026

ABSTRACT

In this paper, numerical and experimental study on flame merging behavior in group fires were carried out. The porous 15cm-square burner was used as a unit burner and propane was employed as a fuel. The burners with various numbers and heat release rates were placed in square configuration with various separation distances. Flame height using video images and temperature distribution with height using thermocouples were measured. The validity of numerical model of FDS (Fire Dynamics Simulator) from NIST (National Institute of Standards and Technology) was confirmed from the comparison with the experimental data. The comparison results show that FDS correctly simulate flame merging behavior in group fire. In addition, the transitional separation distance with frequent flame merging was determined by way of numerical simulation.

Key words: Flame merging behavior, separation distance, group fire, FDS

INTRODUCTION

There are many areas inhabited densely and disorderedly by small buildings in lots of big cities all over the world. Once fires occur in these areas, it is easy to appear group fires. In the city fires emerged after the Great Hansin Earthquake (1995) in Japan, the developments of merged flames or flames affected by nearby flames in the firing zone were observed during the propagation of the city fire, and these flames propagated outward from some fire origins [1]. In fact, these flames in firing zone usually extended to nearby unburned areas through the paths and alleys between many houses, due to the thermal radiation and convection. And then flame merging behavior occurred, which is believed to make the fire more destructive, cause difficulties in fire fighting and often lead to fire whirls.

In spite of the dangerous nature of flame merging behavior, very few literatures are concerned to this study. Sugawa, et al. carried out the experiments with circle burners in 2 by 3 configuration and LPG as fire sources [1], and with various line, square and circle fire sources in many shaped configurations and propane as fuel [2]. They reported the relationship between flame height, and heat release rate and separation distance among fire sources. However, there is no numerical study on flame merging behavior in group fires, which can reduce experimental expenditures and consider more conditions.

Spaces around houses, as well as width and configuration of paths and arrays between houses, and heat release rates of fire sources affect the flame merging behavior and its flame height, which is always deemed to one of the clear indexes to access the fire hazard in the fire fighting being carried out in city fire site. So in this paper, a series of experiments considering various separation distances, numbers and heat release rates of fire sources were conducted. Flame height and temperature distribution with height were measured. Results from numerical simulation on flame merging behavior with LES (Large Eddy Simulation) in FDS are compared with experimental data, and the comparison results are discussed. And then numerical study was carried out to determine the transitional separation distance with frequent flame merging.

EXPERIMENTAL DETAILS

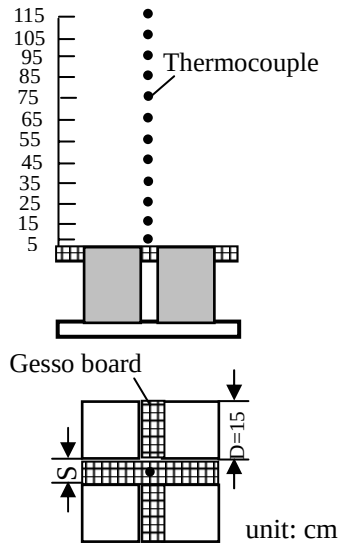

Fig. 1 Elevation and plan views of measuring positions of temperature with 2 by 2 configuration as an example

As shown in Fig. 1 and Fig. 2, square shaped porous diffusion burners of 0.15cm side (D) were located in various square configurations in the still atmosphere. Propane was employed as a fuel, which was supplied to each burner with the control of each flow rate meter. Gesso boards were placed at the height of the burner surface to simulate the ground surface. The heat release rate (Q) of each burner was set as 5.0, 7.5, 10.0, 12.5, 15.0, 17.5 and 20.0kW. Separation distance (S) between burners was chosen as 0, 1, 2, 3cm, representing typical urban block arrangement in densely inhabited area. These values of Q, S and number of burners (N) were changed as experimental and numerical conditions. For fire sources configuration 4×4, the experiments with Q=17.5 and 20.0kW were not conducted due to the large fire leading to out-of-control. And this is also the reason for not carrying out the experiments with 5×5, Q=12.5, 150, 17.5 and 20.0kW. The detailed presentation of the experimental setup can be found in Ref. [3].

Temperature was measured with K-type (chromel-alumel) thermocouples of a diameter of 0.2mm, which were located in the centerline of experimental configuration. Fig. 1 shows the

measuring positions with 2 by 2 configuration as an example. The values reported here of temperature were the average values of 30 data within 60s after the flames were stable. Flames were recorded with digital video, and flame heights were obtained with the average of the 60 visible flame tips height within 30s after the flame were stable.

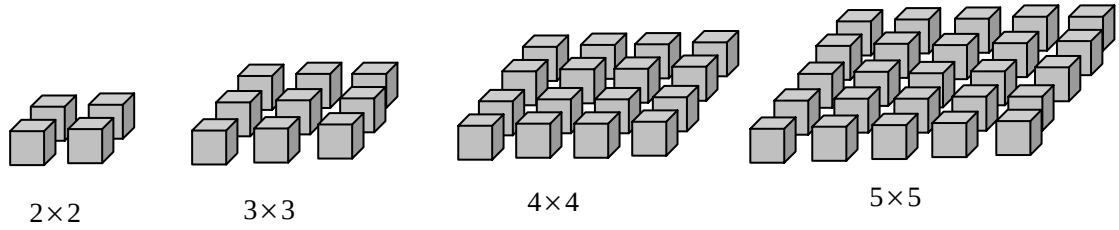

Fig. 2 Fire sources located in various square configurations

NUMERICAL MODELS

Since FDS (Fire Dynamics Simulator) from NIST (National Institute of Standards and Technology) was publicly released in 2000 [4], much experimental work was conducted to validate the models in FDS [5-8]. Throughout its development, FDS has been also proved for providing a tool to study fundamental fire dynamical and combustion.

Here we briefly summarize the models, including hydrodynamics model, combustion model and radiation model used in this study, adopted in the FDS code. Details of these models are supplied in Ref. [4]. In the equations below, all symbols have their usual fluid dynamical meanings, listed in nomenclature in the last section in this paper.

Considering a thermally expandable ideal gas driven by a prescribed heat source, the equations of motion governing the fluid flow, Navier-Stokes equations, are written in a form suitable for low Mach number applications [9-10].

$$\partial\rho/\partial t + \nabla\cdot\rho\vec{u} = 0 \tag{1}$$

$$\partial(\rho Y_l)/\partial t + \nabla\cdot\rho Y_l\vec{u} = \nabla\cdot\rho D_l\nabla Y_l + \dot{m}_l''' \tag{2}$$

$$\rho(\partial\vec{u}/\partial t + (\vec{u}\cdot\nabla)\vec{u}) + \nabla p - \rho\vec{g} = \nabla\cdot\vec{\tau} \tag{3}$$

$$\partial(\rho h)/\partial t + \nabla\cdot\rho h\vec{u} = Dp/Dt - \nabla\cdot\vec{q}_r + \nabla\cdot k\nabla T + \sum_l \nabla\cdot h_l\rho D_l\nabla Y_l \tag{4}$$

These equations as the hydrodynamics model are deduced, simplified and solved numerically. The core algorithm is an explicit predictor-corrector scheme, second order accurate in space and time.

The combustion model is based on mixture-fraction based infinitely fast chemistry kinetics.

The general form of the combustion reaction is:

$$v_O[O] + v_F[F] \rightarrow \sum_P v_P[P] \tag{5}$$

The mixture fraction Z is defined as

$$Z = \frac{sY_F - (Y_O - Y_O^\infty)}{sY_F^\infty + Y_O^\infty}, \quad s = \frac{v_O M_O}{v_F M_F} \tag{6}$$

And the mixture fraction satisfies the conversation law:

$$\rho \frac{DZ}{Dt} = \nabla \cdot \rho D \nabla Z \tag{7}$$

The model assumes that the reactions that consume fuel and oxidizer occur so rapidly that the fuel and oxidizer cannot co-exit. The flame sheet is the location where fuel and oxidizer vanish simultaneously:

$$Z_f = Z_{st} = \frac{Y_O^\infty}{sY_F^\infty + Y_O^\infty} \tag{8}$$

Considering the resolution to capture the combustion and relating dynamics. An effective Z_f is proposed to help the code capture the combusting region:

$$\frac{Z_{f,eff}}{Z_f} = \min(1, C\frac{D^*}{\delta x}) \tag{9}$$

The benefit of the expression $Z_{f,eff}$ is that it provides a quantifiable measure of the grid resolution that takes into account not only the size of the grid cells, but also the size of the fire. And the state relation for oxygen is needed:

$$\text{For} \quad Z < Z_f, \quad Y_O(Z) = Y_O^\infty (1 - Z / Z_{eff}) \tag{10}$$

$$\text{For} \quad Z > Z_f, \quad Y_O(Z) = 0 \tag{11}$$

The heat release rate of per unit volume is based on Huggett's relationship of oxygen consumption [11]:

$$\dot{q}''' = \Delta h_O \dot{m}_O''' \tag{12}$$

Here the oxygen consumption rate is given as:

$$-\dot{m}_O''' = \nabla \cdot (\rho D \frac{dY_O}{dZ} \nabla Z) - \frac{dY_O}{dZ} \nabla \cdot \rho D \nabla Z \tag{13}$$

The radiative transport equation (RTE) for a non-scattering gray gas is

$$r \cdot \nabla I(x,r) = \kappa(x)[I_b(x,r) - I(x,r)] \tag{14}$$

The radiative loss term in the energy equation is

$$-\nabla \cdot q_r(x) = \kappa(x) \cdot [U(x) - 4\pi I_b(x)], \quad U(x) = \int_{4\pi} I(x,r) d\Omega \tag{15}$$

The net radiant energy gained by a grid cell is the difference between that which is absorbed and that which is emitted. The source term is defined as:

$$\kappa I_b = \begin{cases} \kappa\sigma T^4/\pi, outside \\ \chi_r \dot{q}'''/4\pi, inside \end{cases} \quad (16)$$

The radiant heat flux vector q_r is defined as:

$$q_r(x) = \int sI(x,s)d\Omega \quad (17)$$

In this study, a grid sensitivity analysis was performed to determine an appropriate number of cells considering numerical accuracy and computational efficiency. The study is intended to reveal the mesh sensitivity of the predicted flame height. As a test case, the numerical condition with 2 by 2 configuration, S=2cm and Q=15kW was undertaken. The results for these simulations demonstrate that the flame height calculated from meshes consisting of 0.25cm grid cells, 0.50cm grid cells and 0.75cm grid cells, which cost the CPU time with 8.53hr, 4.30hr and 3.67hr, respectively, show very little difference. The computer used for FDS simulation is Dell Dimension 8300 with Pentium IV 2.6GHz and 512M DDR RAM. As a result, for the simulations presented below 0.50cm grid cells was selected. The values of temperature in this simulation were the average values of 30 data within 5s after the flame was stable from the images of heat release rate per unit volume in Smokeview animation. Flame height in this simulation was also obtained with the average flame tips height from the 60 images within 5s of heat release rate per unit volume in Smokeview animation.

RESULTS AND DISCUSSIONS

Comparisons between Numerical and Experimental Results

The size limitation of this paper prevents all of the results being displayed, and so in this paper, only some typical numerical results and experimental data are presented. Fig. 3 shows data sequence of temperature distribution with height (a) and flame height in dimensionless form L_f/D (b) including experimental data and numerical results at fire sources configuration 2×2 with separation distance S=2cm and dimensionless heat release rate Q^*=1.5. Here Q^*= $Q/\rho C_p T_0 g^{1/2} D^{5/2}$, ρ, C_p and T_0 are density, specific heat and temperature of ambient air, respectively, and g is gravitational acceleration. The mean temperature distribution with height and flame height, and their standard deviation were then evaluated. These representative values are tabulated in Table 1. From comparison of the mean experimental flame height and temperature distribution data with height with numerical results, numerical values take on higher in most of data. For the standard deviation of flame height, experimental value is higher than numerical one, because the real flame flickers out and video images only capture discrete values of flame height. However, for numerical one, in fact, the heat release rate per unit volume in Smokeview animation, which is steadier than the real flame, gives the numerical flame height result. The standard deviations of experimental

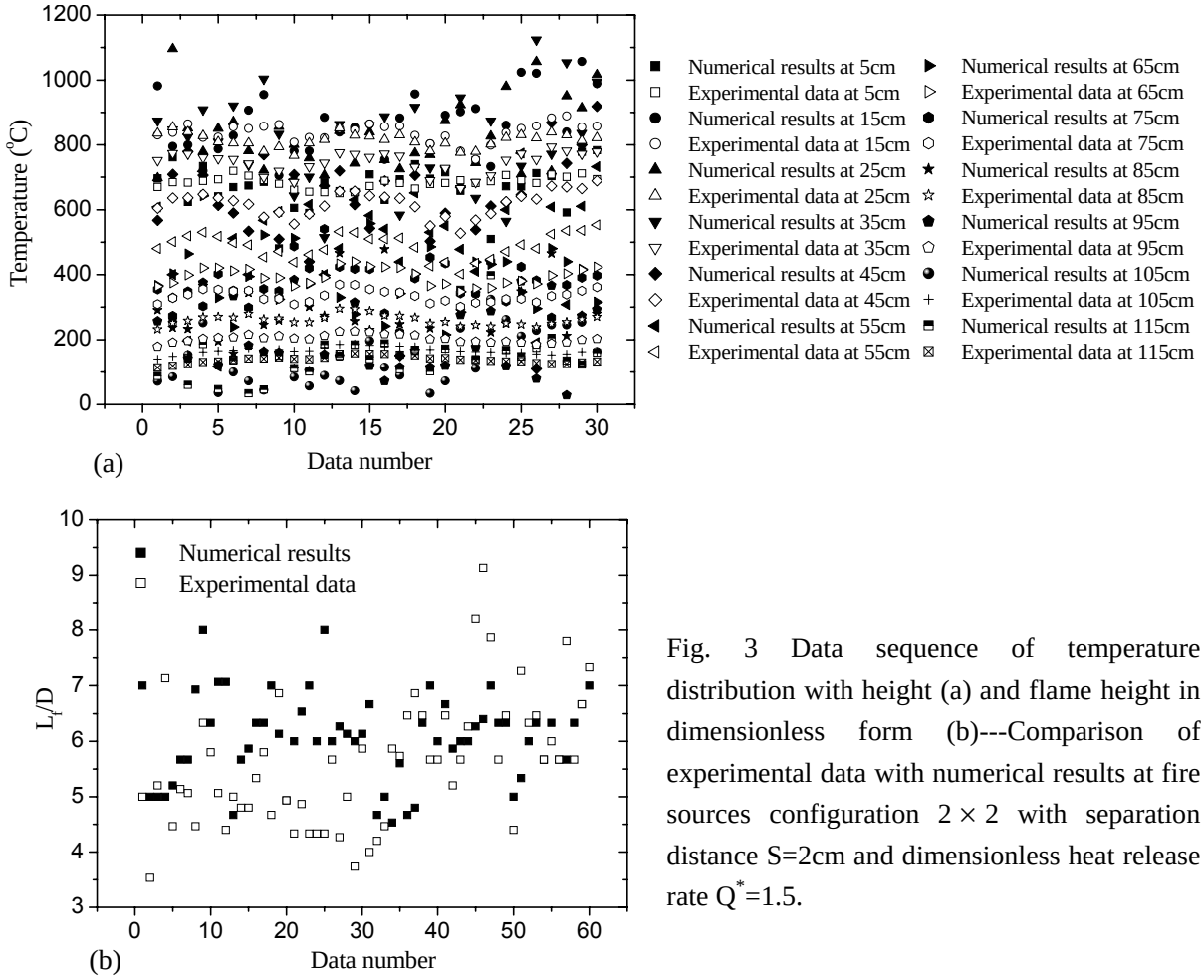

Fig. 3 Data sequence of temperature distribution with height (a) and flame height in dimensionless form (b)---Comparison of experimental data with numerical results at fire sources configuration 2×2 with separation distance S=2cm and dimensionless heat release rate Q^*=1.5.

Table 1 Mean and standard deviation of flame height and temperature distribution with height at fire sources configuration 2×2 with separation distance S=2cm and dimensionless heat release rate Q^*=1.5.

	Flame height (cm)	Temperature (°C)											
		5 cm	15 cm	25 cm	35 cm	45 cm	55 cm	65 cm	75 cm	85 cm	95 cm	105 cm	115 cm
Numerical mean	90.8	672	861	831	813	621	513	390	373	269	205	156	154
Experimental mean	84.0	684	838	814	745	619	489	394	335	261	203	166	138
Numerical std.	11.9	70	98	108	147	172	161	99	69	92	106	101	79
Experimental std.	17.5	18	19	23	34	40	38	26	19	16	12	11	12

temperature data are much less than that of numerical results. The reason results in this is that thermocouples have the respective response times, and in fact the experimental temperature data are the average values of some time. Despite this, the numerical results accord relatively well with the experimental data considering the numerical model limitation and the experimental precision.

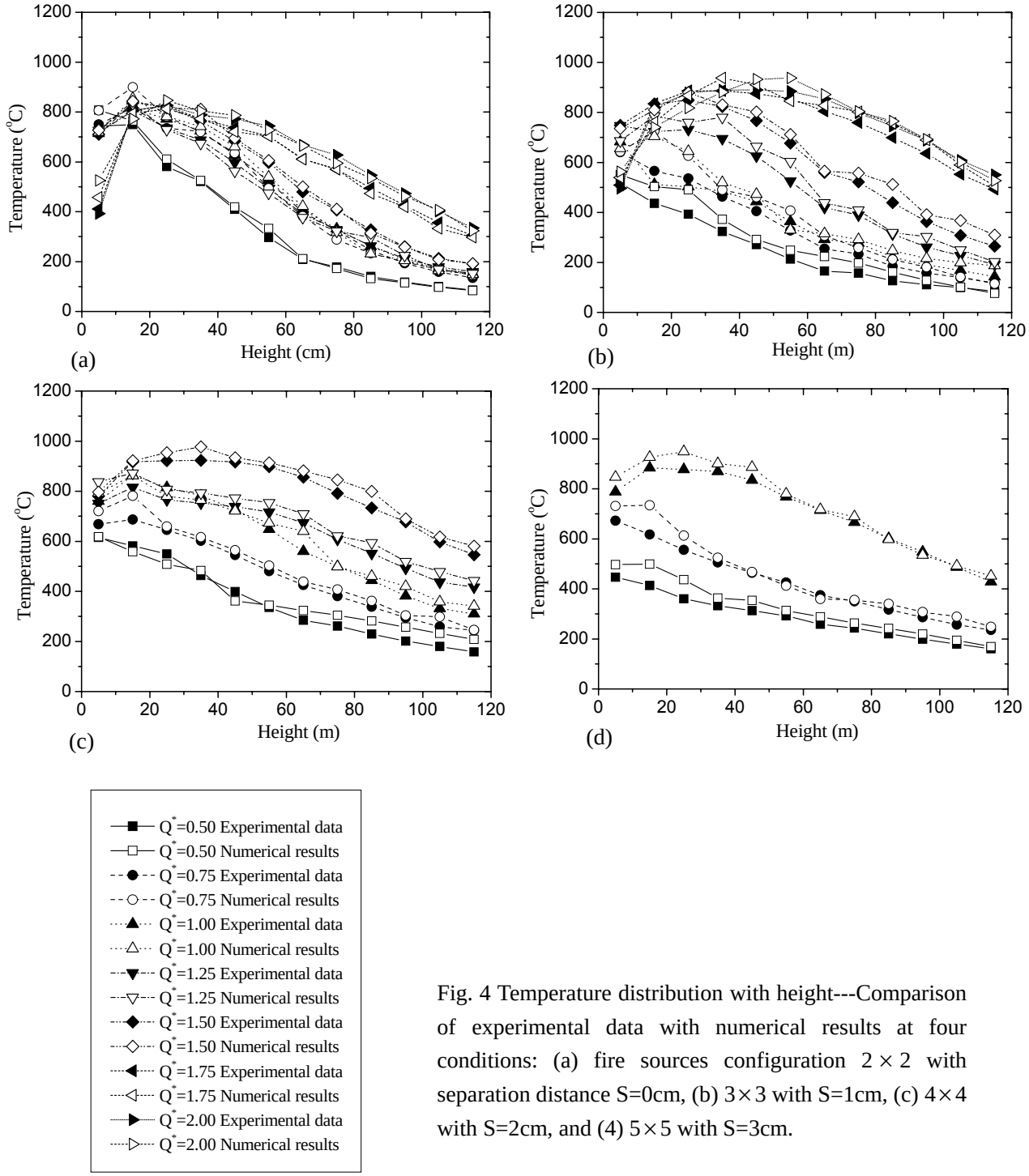

Fig. 4 Temperature distribution with height---Comparison of experimental data with numerical results at four conditions: (a) fire sources configuration 2×2 with separation distance S=0cm, (b) 3×3 with S=1cm, (c) 4×4 with S=2cm, and (4) 5×5 with S=3cm.

The results of the preliminary assessments of how well the flame merging behavior in group fires is simulated are shown in Fig. 4 and 5. Fig. 4 is the experimental data and numerical results of temperature distribution with height at four conditions: (a) fire sources configuration 2×2 with separation distance S=0cm, (b) 3×3 with S=1cm, (c) 4×4 with S=2cm, and (4) 5×5 with S=3cm. From the first view, the numerical results are close to the corresponding experimental data. But in most of data, predicted temperatures are higher than

measured temperatures, which results from the mixture fraction combustion model in FDS. This model is based on the assumption that the combustion is mixing-controlled, which means the combustion occurs much more rapidly than the resolvable convective and diffusive phenomena. From Fig. 4, the result that the more heat release rate each burner leads to the higher temperature is obtained. The temperature distribution with the more heat release rate each burner, increases with height initially, and then decrease. But for the less one, the temperature distribution always decreases with height.

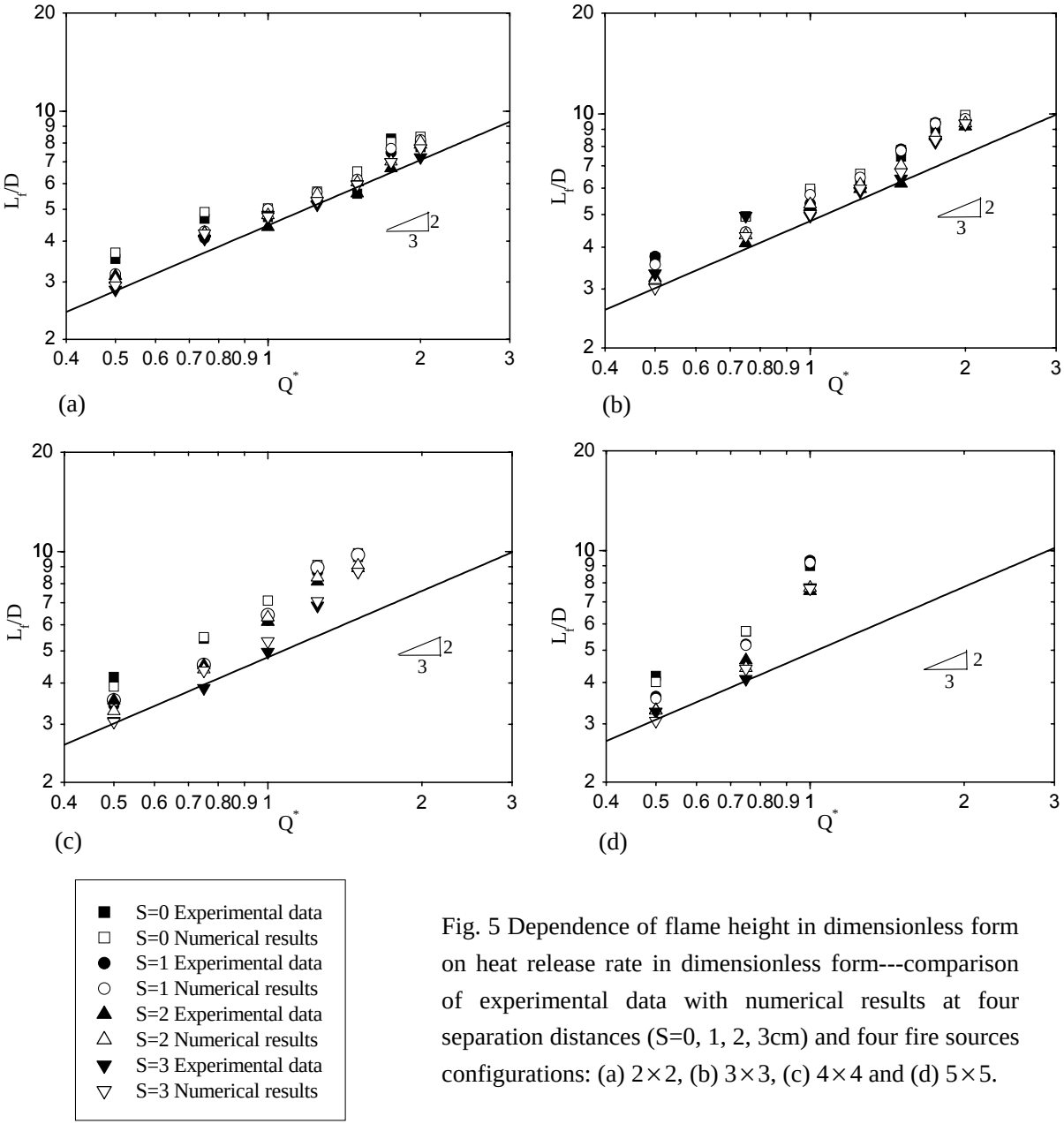

Fig. 5 Dependence of flame height in dimensionless form on heat release rate in dimensionless form---comparison of experimental data with numerical results at four separation distances (S=0, 1, 2, 3cm) and four fire sources configurations: (a) 2×2, (b) 3×3, (c) 4×4 and (d) 5×5.

Fig. 5 indicates the comparison of experimental data with numerical results of dependence of flame height in dimensionless form on heat release rate in dimensionless form at four separation distances (S=0, 1, 2, 3cm) and four fire sources configurations: (a) 2×2, (b) 3×3,

(c) 4×4 and (d) 5×5. The power correlation between dimensionless flame height and dimensionless heat release rate is not the same as the result from Ref. [2], $L_f/D \propto Q^{*2/5}$, for square fire source. The power value of 2/3 is appropriate for fire sources configuration 2×2 and 3×3, and the higher values for 4×4 and 5×5 are obtained not only from experimental data, but also numerical results. The reasons are not clear now, but maybe more fire sources result in this. From Fig. 5, it is indicated that the numerical results accord well with the experimental data. So FDS correctly predicts flame height and temperature distribution with height in simulating flame merging behavior in group fires.

The power correlation between dimensionless flame height and dimensionless heat release rate, 2/3 or higher values from Fig.5, is believed to be a result of the flame merging effect. It is also obvious that the more fire sources cause the higher power values. Comparing Fig. 5(a) with Fig. 5(b)-(d), with the same of heat release rate each burner, the more fire sources lead to the higher flame height. And with the same of fire sources configuration, the more heat release rate also result in the higher flame height. So in order to control the occurrence of flame merging behavior in group fire, it is necessary to decrease heat release rate each burner and number of fire sources.

Transitional Separation Distance with Frequent Flame Merging

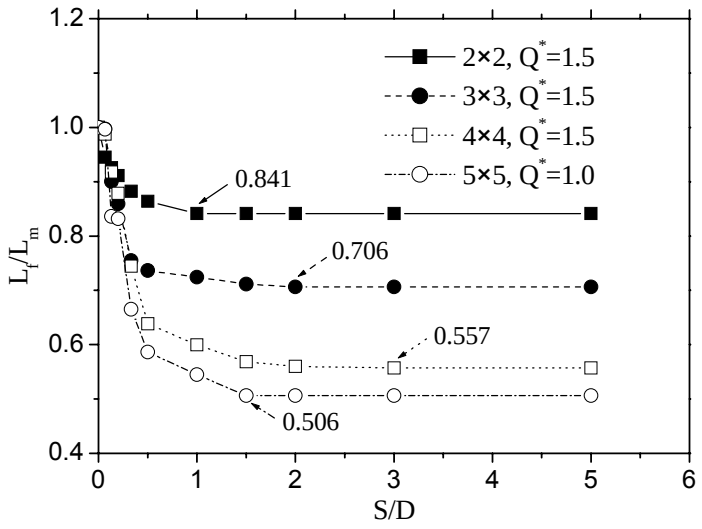

Fig. 6 Dimensionless flame height merged as a function of dimensionless separation distance at four conditions: fire sources configuration 2×2 with dimensionless heat release rate Q^*=1.5, 3×3 with Q^*=1.5, 4×4 with Q^*=1.5 and 5×5 with Q^*=1.0.

If separation distance between burners S increase keeping the heat release rate each burner constant, flame will transfer from merged flame to flame as single burner. This can be demonstrated by Fig. 6, dimensionless flame height merged L_f/L_m, as a function of dimensionless separation distance S/D, at four conditions: fire sources configuration 2 × 2 with dimensionless heat release rate Q^*=1.5, 3×3 with Q^*=1.5, 4×4 with Q^*=1.5 and 5×5 with Q^*=1.0. Here, L_m is the flame height with no separation at the corresponding conditions, and the values of L_m in Fig. 6 are 98.12, 116.87, 148.19 and 138.48cm at 2×2 with Q^*=1.5, 3×3 with Q^*=1.5, 4×4 with Q^*=1.5 and 5×5 with Q^*=1.0, respectively.

It is obvious from Fig. 6 that with the increase of S/D, L_f/L_m decreases, but reaches a certain value at a separation distance. In this separation distance, flames are sometimes merged and sometimes apart as the flames from a single burner. And so this separation distance is called

as transitional separation distance with frequent flame merging. The reason results in this is that when separation distance reaches a transitional value, the air entrained by the flame is enough to sustain the structure of flame, and so the flame does not lean in and merge together. Fig. 6 also shows that the transitional separation distances at various conditions are different. The more burners with the same heat release rate each burner lead to the longer transitional separation distances, which result in the lower dimensionless flame height. This is because the more burners need the more air supply, caused by the longer transitional separation distance. Also the lower heat release rate each burner need the less air supply, caused by the shorter transitional separation distance.

CONCLUSIONS AND FUTURE WORK

This paper presents the numerical results and experimental data on flame merging behavior in group fires. FDS was used to simulate flame merging behavior. Comparisons of flame height and temperature distribution with height between numerical results and experimental data were carried out. In this paper, the transitional separation distance with frequent flame merging was also determined with numerical results. The main conclusions are listed below:
(1) The power correlation between dimensionless flame height and dimensionless heat release rate is $L_f/D \propto Q^{*2/3}$, for square fire sources configuration 2×2 and 3×3, and the power values for 4×4 and 5×5 are higher.
(2) With the same of heat release rate each burner, the more fire sources lead to the higher flame height. And the more heat release rate also result in the higher flame height with the same of fire sources configuration.
(3) FDS correctly predicts flame height and temperature distribution with height in simulating flame merging behavior in group fires.
(4) The more burners with the same heat release rate each burner lead to the longer transitional separation distances with frequent flame merging, which result in the lower dimensionless flame height.

Since FDS can be used to predict flame merging behavior in group fires, to determine the details of the merged flame structure with FDS is future work. Why forms merged flame in group fire, i.e. the formation mechanism, will be also studied. A simple or empirical model to predict the flame height of merged flame is another future work because flame height is an important parameter for assessing the fire hazard.

ACKNOWLWDGMENTS

The authors would like to acknowledge the support provided by the Japan Society for the Promotion Science Postdoctoral Fellowship (Grant No. 03246) and the National Natural Science Foundation of China (Grant No. 50306024). The experiments were conducted at the Building Research Institute, Tsukuba, by the support of the National Institute of Land and

Infrastructure Management, MLIT.

NOMENCLATURE

C	constant to adjust the stoichiometric mixture for grid size
c_p	specific heat of air (J/kgK)
D	diffusion coefficient (m^2/s)
D_l	diffusion coefficient of lth species (m^2/s)
D^*	the local characteristic length with reference to grid size (m)
$\vec{g}$	acceleration of gravity (m/s^2)
h	enthalpy (J)
h_l	enthalpy of lth species (J)
I	radiation intensity (J/m^2)
I_b	radiation blackbody intensity (J/m^2)
k	thermal conductivity (W/mK)
$\dot{m}_l'''$	mass rate per unit volume of lth species (kg/m^3s)
$\dot{m}_O'''$	mass rate per unit volume of oxygen (kg/m^3s)
p	pressure (kg/m^2)
$\dot{q}'''$	heat release rate per unit volume (w/m^3)
$\vec{q}_r$	radiative heat flux vector (W/m^3K)
s	stoichiometric oxygen/fuel mass ratio
t	time (s)
T	temperature (K)
U	integrated radiant intensity (W/m^2)
$\vec{u}$	velocity vector (m/s)
Y_F	mass fraction of fuel
Y_l	mass fraction of lth species
Y_O	mass fraction of oxygen
Z	mixture fraction
Z_f	averaged mixture fraction at flame tip
$Z_{f,eff}$	effective mixture fraction at flame tip
Z_{st}	stoichiometric mixture fraction at flame tip
Δh_O	energy released per unit mass oxygen consumed (J/kg)
κ	absorption coefficient (m^{-1})
ρ	density (kg/m^3)
$\vec{\tau}$	viscous stress tensor (kg/ms^2)

σ stenfan-boltzmann constant (J/m^2K^4)

REFERENCES

1. Sugawa, S. and Oka, Y. Experimental Study on Flame Merging Behavior from 2 by 3 Configuration Model Fire Sources. Fire Safety Science—Proceedings of the Seventh International Symposium, Massachusetts, USA. 2002, pp. 891-903.
2. Sugawa, S., Satoh, H. and Oka, Y. Flame Height from Rectangular Fire Sources Considering Mixing Factor. Fire Safety Science—Proceedings of the Third International Symposium, Edinburgh, Scotland, 1991, pp. 435-444.
3. Fukuda, Y. Kamikawa, D., Hasemi, Y. and Kagiya, K. Flame Characteristics of Group Fires. Proceedings of the Second International Symposium on New Technologies for Urban Safety of Mega Cities in Asia. Tokyo, Japan, 2003, pp.119-124.
4. McGrattan, K.B., Baum, H.R., Rehm, R.G., Hamins, A. and Forney, G.P. Fire Dynamics Simulator. Technical Reference Guide. Technical Report NISTIR 6467, National Institute of Standards and Technology, Gaithersburg, Maryland, 2000.
5. Clement, J.M. and Fleischmann, C.M. Experimental Verification of Fire Dynamics Simulator Hydrodynamic Model. Fire Safety Science—Proceedings of the Seventh International Symposium, Massachusetts, USA. 2002, pp. 839-850.
6. Friday, P.A. and Mowrer F.W. Comparison of FDS Model Predictions with FM/SNL Fire Test Data. NIST GCR 01-810, National Institute of Standards and Technology, Gaithersburg, Maryland, 2001.
7. Petterson, N.M. Assessing the Feasibility of Reducing the Grid Resolution in FDS Field Modeling. Fire Engineering Research Report 2002/6, University of Canterbury, 2002.
8. Ma, T.G. and Quintiere, J.G. Numerical Simulation of Axi-symmeric Fire Plumes: Accuracy and Limitations. Fire Safety Journal, 2003, 38: 467-492.
9. Baum H.R., McGrattan, K.B., and Rehm, R.G. Three Dimensional Simulations of Fire Plume. Fire Safety Science—Proceedings of the Fifth International Symposium, Tsukuba, Japan, pp. 511-522.
10. McGrattan, K.B., Baum, H.R., Rehm, R.G., Hamins, A. et al. Fire Dynamics Simulator (Version 4)--Technical Reference Guide. Technical Report NISTIR 6783, National Institute of Standards and Technology, Gaithersburg, Maryland, 2003.
11. Huggett, C. Estimation of the Rate of Heat Release by Means of Oxygen Consumption Measurements. Fire and Materials, 1980, 4: 61-65.